Fuel 228 (2018) 297–308

Contents lists available at ScienceDirect

Fuel

journal homepage: www.elsevier.com/locate/fuel

Full Length Article

A comparative study on the mineralogy, chemical speciation, and combustion behavior of toxic elements of coal beneficiation products

Biao Fu[a,b], Guijian Liu[a,b,*], Mei Sun[a], James C. Hower[c], Guangqing Hu[a,d], Dun Wu[a,d]

[a] CAS Key Laboratory of Crust-Mantle Materials and Environment, School of Earth and Space Sciences, University of Science and Technology of China, Hefei, Anhui 230026, China
[b] State Key Laboratory of Loess and Quaternary Geology, Institute of Earth Environment, The Chinese Academy of Sciences, Xi'an, Shaanxi 710075, China
[c] University of Kentucky, Center for Appl Energy Research, 2540 Research Park Drive, Lexington, KY 40511, United States
[d] Exploration Research Institute, Anhui Provincial Bureau of Coal Geology, Hefei, Anhui 23008, China

ARTICLE INFO

Keywords:
Preparation plant wastes
Toxic elements
Mineralogy
Modes of occurrences
Volatility

ABSTRACT

The huge demand for high-quality coal in China has resulted in increased generation of preparation plant wastes of various properties. A series of beneficiation products collected from a preparation plant were characterized to understand their petrographic and mineralogical characteristics, as well as thermochemical and trace element behavior during combustion. The minerals in the Luling preparation plant wastes from Huaibei coalfield mainly included kaolinite and quartz, with minor calcite, ankerite, pyrite, illite, chalcopyrite, albite, K-feldspar, anatase/rutile, and iron-oxide minerals. Massive clay lumps of terrigenous origin, cleat-infilling carbonate, and pyrite of epigenetic origin were prone to be enriched in the middlings and coal gangue. Minor or trace heavy minerals also reported to the preparation plant wastes. The contents of low-density density vitrinite and liptinite were enhanced in the clean coal, while inertinite-maceral group were enriched in the middlings. The modes of occurrences of toxic elements differed between raw coal and the waste products; and their transformation behavior during heavy medium separation is largely controlled by clay minerals (V, Cr, Co, Sb, and Pb), carbonate minerals (Co and Pb), sulfide minerals (As, Cu, Ni, Cd, and Zn) and organic matters (V, Cr, Se, and Cu). Three groups were classified based on the volatile ratio (Vr) of toxic elements. Group 1 includes the highly volatile element Se with Vr > 85%; Group 2 contained elements As, Pb, Zn, Cd and Sb, with the Vr in the range of 20–85% and V, Cr, Co, Ni and Cu with Vr less than 20% were placed into Group 3. Thermal reactivity of coal inferred from the combustion profiles could be significantly improved after coal beneficiation, whereas the increased inorganic components probably inhibited the thermal chemical reaction of wastes.

1. Introduction

To upgrade the quality of coal for industrial utilization, the ratio of cleaned coal to raw coal in China has rapidly increased in the past decades. According to statistics up to 2011, the total amount of preparation plant rejects is more than 3 Gt in China. It has been well-documented that toxic trace elements in coal were prone to be associated with mineral matter, especially for high-ash coal with large amounts of heavy-metal-bearing minerals such as pyrite, barite, rutile/anatase, among others [1–5]. Minerals such as clay and pyrite in coal are targeted for removal in coal preparation to reduce the sulfur, mineral matter, and associated toxic trace elements [6–9]. Different types of coal preparation plant rejects show wide variations in physiochemical properties, such as ash yield, moisture content, maceral distribution, mineral compositions, etc. [9–11]. Recently, much attention has been paid to the research and application of three-product dense medium cyclones (DMCs) in China [12,13]. The waste product types produced from the DMCs (Fig. 1) include high-ash coal gangue, fine middling coal, and coal slime of ultrafine coal with high water contents. However, there are only a few works focusing on the petrologic, mineralogical and geochemical characteristics of different coal beneficiation products generated from DMCs units in coal preparation plants [11,14]. In addition, while correlations between element partitioning and physical separations are usually used as the basis to infer the elemental associations [9,10], data on the chemical speciation of trace elements in individual beneficiation products are still lacking.

On the other hand, the cleaning wastes contain combustible materials which could be used in electricity generation and are regarded as a

* Corresponding author at: CAS Key Laboratory of Crust-Mantle Materials and Environment, School of Earth and Space Sciences, University of Science and Technology of China, Hefei, Anhui 230026, China.
E-mail address: lgj@ustc.edu.cn (G. Liu).

https://doi.org/10.1016/j.fuel.2018.04.085
Received 14 January 2018; Received in revised form 10 April 2018; Accepted 17 April 2018
Available online 04 May 2018
0016-2361/

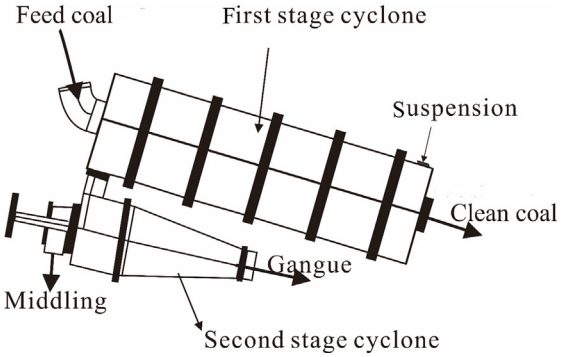

Fig. 1. Sketch map of three-product DMCs (3GDMC1200/850A) in Luling preparation plant, based on the data provided by the local technicians.

potentially valuable energy resource [15–18]. Some countries such as Australia [17,18], India [19], and China [20] have developed fluidized-bed combustion (FBC) technology as a means for recovering energy from preparation plant wastes. Thermogravimetric analysis (TGA) has been extensively used in studying the reactivities of carbonaceous materials to assess the thermochemical properties of coal, biomass, and so on [21,22]. The combustion profile of TGA depends upon various parameters such as coal rank, maceral distribution, and mineral contents. In addition, due to the enrichment of some toxic elements in the high-ash waste products, the volatile characteristics of the elements during preparation plant wastes combustion could be of concern. The volatility of toxic trace elements is mainly a function of modes of elemental occurrences and combustion conditions [23,24,26,28–30]. Differences in maceral composition, coal rank, and mineral matter of preparation plant wastes may result in different combustion reactivities and volatile tendencies of toxic elements [25,26].

The objectives of this study were to use multidisciplinary means to investigate (a) the petrology, mineralogy, and geochemistry of various preparation plant wastes produced from DMC, (b) thermal characteristics of cleaning wastes via thermal gravimetric analysis, and (c) volatile characteristics of toxic elements during coal cleaning waste combustion. The results of this study are expected to provide a useful basis for treating the cleaning waste products in an environmentally friendly and economical manner.

2. Materials and methods

2.1. Background and sample collection

In this study, a series of samples including raw coal, middlings, clean coal, slime, and coal gangue were sequentially collected from the DMCs of Luling coal preparation plant in the Huaibei coalfield (Fig. 1). The feed coal in the plant all came from the coal seams 8, 9 and 10 of Luling mine of Huaibei coalfield. The heavy dense medium used in the DMC unit was mainly composed of magnetite powder. As shown in Fig. 1, during the cleaning process, the feed consisted of blended coal and dense medium that enters tangentially near the top of the cylindrical section of the cyclone can form a strong swirling flow .Due to the centrifugal forces, heavy fractions of parent coal with high specific gravity should move towards the wall and discharge in the underflow through the spigot, while light fractions could be caught in an upward stream and generated clean coal from the overflow outlet [27]. The suspended liquid that contained 0.25–2.0-mm coal particles generated from the overflow will enter into the slime dense medium cyclones, which can recover the clean coal and produce tailings. Coal slurry produced from the whole process of DMC will enter into the flotation cell to recover the clean coal, and the tailing slurry will be concentrated and then dewatered by centrifuges and filter press. The resulting three cleaning products (clean coal, middlings, and gangue) were screened to recover the medium and yielded the final products. DMCs in the Luling preparation plant can process raw coal at 3 Mt/a. The gangue, middlings, and slime were generally used for generating electricity in the local power plants [28], occasionally the coal gangue was used as a raw material in a brick-making plant [29].

All the samples were homogenized and reduced to obtain a representative 2–3 kg sample, and then were immediately sealed into plastic bags to avoid possible oxidation and contamination. Each sample was dried at 40 °C for 24 h, and then crushed in an agate mortar to pass through the 60-mesh sieve for different experiments.

2.2. Analytical methods

The contents of C, H, and N in the sample were determined using an elemental analyzer (Vario EL cube). Proximate analysis (ash yield, moisture, and volatile matter) was analyzed based on ASTM Standards D3174-04, D3173-04 and D3175-04 (ASTM, 2007), respectively. Total sulfur and forms of sulfur were determined following ASTM Standards D3177-02 and D2492-02 (ASTM, 2007), respectively. Petrographic analysis of all samples was performed at the University of Kentucky Center for Applied Energy Research. Each sample was ground to less than 1 mm and prepared as epoxy-bound pellet and examined with 50× oil-immersion reflected-light optics using Leitz Orthoplan microscopes. The mineralogical phases in the waste products were determined by X-ray powder diffraction, supplemented by examination using a field emission scanning electron microscope (TESCAN MIRA3 LMH Schottky FE-SEM), equipped with an energy dispersive analysis system of X-ray (EDAX, Genesis APEX Apollo System). The XRD analysis of each sample was carried out on a Phlips X'Pert PRO X-ray powder diffraction with Cu K-alpha radiation, and the patterns are recorded over a 2θ interval of 3–70°, with a step increment of 0.02°. The working distance of the SEM was about 10 mm with beam voltage 15 or 20.0 kV. Samples were carbon coated and then were mounted on aluminum SEM stubs using sticky conductive tapes.

2.3. Chemical analysis

The major element oxides were determined by XRF (XRF-1800). Before XRF analysis, all the samples were ashed at a temperature of 815 °C, an alkaline fusion method for the high temperature ash were employed prior to the XRF analysis. The loss-on-ignition (LOI) was also determined at 815 °C [31]. Trace elements in the samples were determined by ICP-MS (Thermo Fisher, X Series II), and As and Se were determined using AFS (AFS-230Q). Approximately 0.05 g of each powder sample (200-mesh) was transferred into a PTFE digestion vessel with 2-ml purified HNO_3 overnight, and then added to an acid mixture (HNO_3: HF = 2:5) in a programmed microwave oven (from room temperature to 120 °C in 10 min and kept for 10 min; then increased to 160 °C in 5 min and kept for 10 min; finally increase to 210 °C and kept for 60 min). Finally, each solution was filtered through a 0.45-μm membrane and made up to 25-ml with Milli-Q water with 3% HNO_3. Two percent HNO_3 solution was injected into the ICP-MS system to eliminate the memory effect of the previous sample. The Re internal standard solution was used for tuning and checking of the ICP-MS calibration, obtaining a RSD lower than 8%. Blanks, certified reference materials SARM-20 (coal) and GBW07406 (soil) were digested and determined following the same procedure used for checking the accuracy of the trace elements. Analytical errors were less than 5% for most elements and around 10% for V (108.3%), and Pb (106.2%).

A six-step sequential chemical extraction (SCE) was used to determine the modes of occurrences of trace elements in the coal waste samples. The SCE procedural separates the trace elements into six fractions: water-leachable, ion-exchangeable, carbonate-bound, organic-bound, silicate-bound, and sulfide-bound. The detailed SCE procedure for toxic elements (V, Cr, Co, Ni, Cu, Zn, As, Cd, Se, Pb, and Sb) of environmental concern in the samples was based on Dai et al. [32].

Briefly, the water-soluble associated elements were leached from the 4-g samples with 30-ml Milli-Q water; then the residues were mixed with 1 M NH_4Ac to extract the elements bound with ion-exchangeable fractions. After drying the residues at 40 °C for 8 h, the organic matter and minerals in the residues were separated by $CHCl_3$(1.47 g/cm^3). The floating organic matter was digested using HNO_3 + $HClO_4$ and the carbonate minerals in the residues were dissolved by HCl. Finally, the silicate- and sulfide-bound associations were separated by the $CHBr_3$(2.89 g/cm^3), and then the HF and HNO_3 were added for extracting the silicate-associated trace elements and HNO_3 was used for dissolving the sinking sulfide-associated residues.

2.4. Combustion procedural and thermal analysis

Thermal-chemical characteristics of coal cleaning wastes and cleaning coal were determined by a Thermal Analyzers (SDT Q600). The sensitivity of the microbalance was 0.1 μg and the precision of temperature measurement was 0.1 °C, with the heating rate ranging from 0.1 to 100 °C/min. To avoid the mass and heat transfer interference, around 15 mg sample was loaded into the Al_2O_3 crucible and heating under a 100 ml/min air flow from room temperature to 1000 °C at heating rate of 15 °C/min. The TG-DTG curves were obtained in order to investigate the combustion characteristics of the samples.

Simulated combustion of the coal and corresponding products was conducted in a vacuum tube furnace to determine the volatile characteristics of toxic trace elements [30]. Generally, each powder sample (5 g) was fed into the furnace slowly when the temperature reached 950 °C under constant air flow with residence time of half an hour. After cooling down, the combustion residues were sent for the trace elements analysis. The solid residue samples were ground to less than 75 μm, digested, and analyzed following the same experiment procedure for trace element determination as indicated in Part 2.3.

3. Results and discussion

3.1. Proximate and ultimate analysis

The results of proximate and ultimate analysis of cleaning products coal are given in Table 1. Raw coal fed into the preparation plant is a medium volatile bituminous coal ($R_{o,ran}$ = 1.1%), characterized by low moisture (1.4%) and moderate ash yield (23.6%). The coal quality parameters of the raw coal are consistent with the Huaibei coals [33,34]. The ash yield of the preparation products followed the decreasing order: gangue (84.6 wt%) > middlings (41.3% wt%) > slime (34.6 wt%) > clean coal (7.9 wt%), indicating a high efficiency of the cleaning process. The content of carbon (C), hydrogen (H), and nitrogen (N) exhibits a contrasting difference between cleaning coal and waste products. However, variations of sulfur contents do not show any significant trends between raw coal and its beneficiation products, which can be ascribed to the dominant organic sulfur in the raw coal. Forms of sulfur analysis indicate that the sulfides can be efficiently reduced by the DMCs separation process and consequently enriched in the preparation plant wastes (middlings and coal gangue).

Table 1
Proximate and ultimate analysis (%), and forms of sulfur (%) of the samples of the raw coal and cleaning products from Luling preparation plant.

Sample	Parameters	Raw coal	Middlings	Clean coal	Slime	Gangue
Proximate analysis	M_{ad}	1.40	1.12	1.44	0.93	nd
	V_{daf}	36.08	29.78	35.6	30.33	nd
	A_d	23.61	41.30	7.91	34.58	84.63
Ultimate analysis	C_{ad}	61.84	44.57	70.26	53.26	10.72
	H_{ad}	4.10	3.13	5.17	3.49	1.58
	N_{ad}	1.12	0.76	1.26	0.94	0.18
Forms of Sulfur	$S_{t,d}$	0.57	0.68	0.64	0.60	0.64
	$S_{p,d}$	0.10	0.26	0.06	0.14	0.22
	$S_{s,d}$	0.04	0.03	0.02	0.02	0.08
	$S_{o,d}$	0.43	0.39	0.56	0.44	0.34

"nd": not determined; M: Moisture; V: volatile matter; A: ash yield; C: carbon; H: hydrogen; N: nitrogen; S_t: total sulfur; S_p: pyritic sulfur; S_s: sulfate sulfur; S_o: organic sulfur; ad: air-dried basis; d: dry basis; daf: dry and ash-free basis

3.2. Petrographic and mineralogical characterization

The maceral assemblages are mainly composed of vitrinite and inertinite. On the mineral- free basis, vitrinite-maceral groups are dominated by collotelinite and collodetrinite (Table 2). The inertinite in the raw coal consists mainly of fusinite and semifusinite, along with minor micrinite. The liptinite is mainly represented by sporinite (Fig. 2E). Clay, carbonate, and pyrite are the visible minerals observed by optical microscopy (Fig. 2).

A comparison of petrographic components between raw coal and washing products can be seen in Table 2. The content of vitrinite is much lower in the middlings (43.4 vol.%) than that in raw coal (61.0 vol.%) while inertinite increased from 32.5 vol.% of raw coal to 51.1 vol.% of middlings. In comparsion to raw coal, clean coal exhibits opposite trends for maceral distribution, having relatively higher vitrinite and liptinite contents but lower inertinite contents. The petrographic characteristics of slime are similar to that of the raw coal. The different physiochemical properties of coal macerals may determine their partitioning behavior during DMCs process. For example, brittle vitrinite having lower density will report to fine particle and light fractions whereas high-density mineral matter and inertinite components tend to report to coarse sizes and heavier fraction [35,36]. It was difficult to do the point counting work on the gangue for petrographic analysis, owing to its low contents of the maceral components. It was observed that the primary petrographic components in coal gangue were clays and other accessory minerals. Maceral constituents, such as inertinite, in gangue are usually fragmented into small, dispersed debris mixed with clays (Fig. 2D).

The results of minerals determined by XRD, reflected light

Table 2
Petrographic analysis results determined under the optical microscopy for raw coal and beneficiation products (vol.%; on a mineral-free basis).

	Raw coal	Middlings	Clean coal	Coal slime
Telinite	0.6	0	0.4	0.7
Collotelinite	28.5	15.1	32.6	22.8
Total telovitrinite	29.1	15.1	33	23.5
Vitrodetrinite	1.8	3.3	2	6.2
Collodetrinite	29.7	25	30.5	27.1
Total detrovitrinite	31.5	28.3	32.4	33.3
Corpogelinite	0.4	0	0.2	0
Gelinite	0	0	0	0
Total gelovitrinite	0.4	0	0.2	0
Total vitrinite	61.0	43.4	65.6	56.8
Fusinite	14.4	27.9	11.4	14
Semifusinite	12.8	15.4	4.5	10.6
Micrinite	3.3	1.1	2.9	2.4
Macrinite	0.6	0.4	2.6	3.1
Secretinite	0.2	0	0.2	0.4
Funginite	0	0	0	0
Inertodetrinite	1.2	6.3	3.1	5.5
Total inertinite	32.5	51.1	24.8	36.1
Sporinite	5.1	4	5.7	2.7
Cutinite	0.6	0.7	1.2	2
Resinite	0	0.7	1	0.4
Alginite	0	0	0	0
Liptodetrinite	0.6	0	1.4	0.9
Suberinite	0.2	0	0.4	1.1
Exsudatinite	0	0	0	0
Total liptinite	6.5	5.5	9.6	7.1

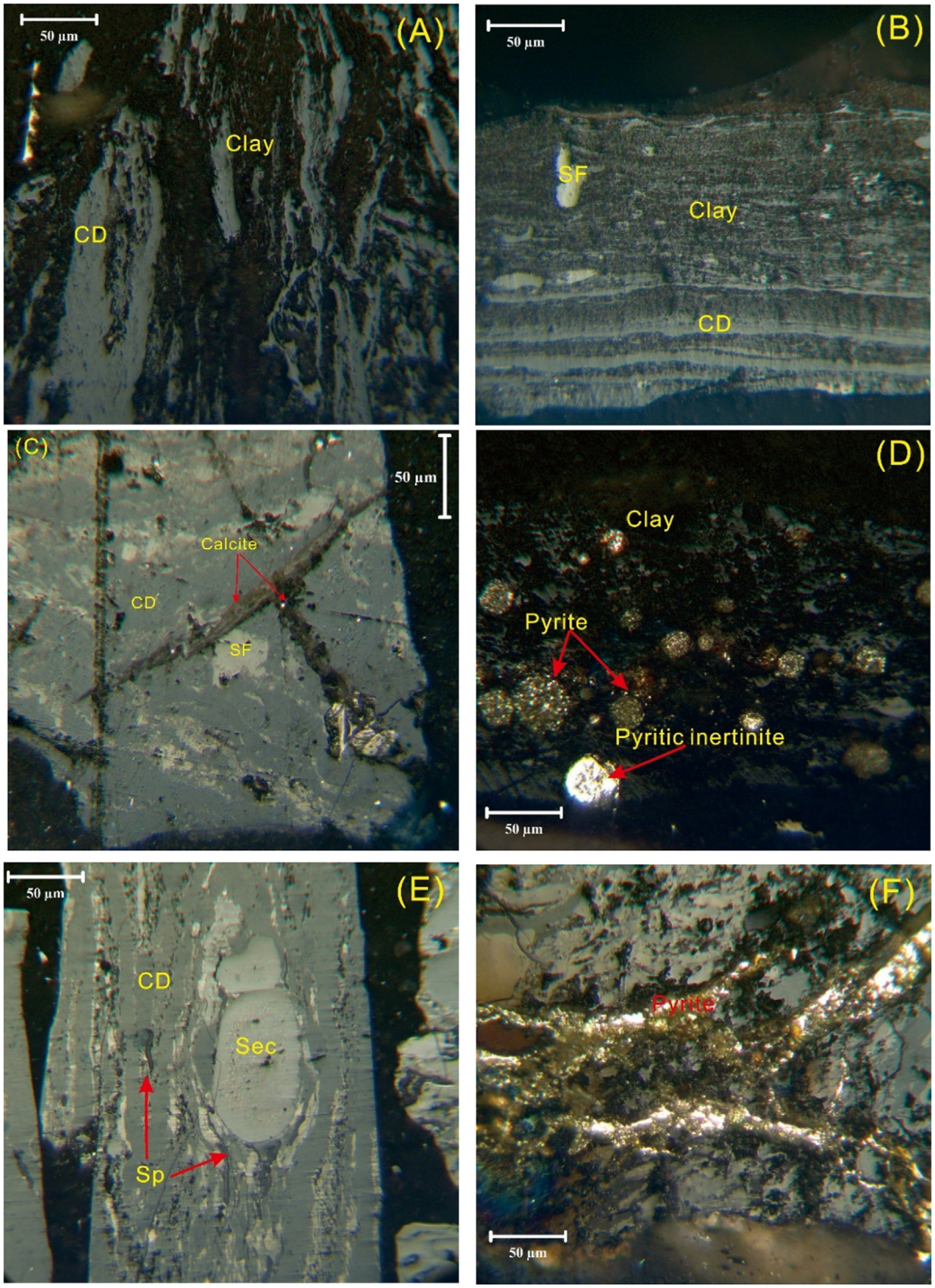

Fig. 2. Petrographic characteristics of raw coal and beneficiation products. (A) Massive lumps of clay distributed along the bedding plane of collodetrinite (CD) in middlings. (B) Clay bands distributed in the collodetrinite (CD) in clean coal. (C) cleat-infillings of calcite in middlings. (D) framboidal pyrite embedded into the clay and vitrinite in coal gangue. (E) Secritinite (Sec), sporinite (Sp), and collodetrinite (CD) in raw coal. (F) fracture-filling pyrite, vitrinite, and semifusitie in middlings.

microscopy, and SEM-EDX in raw coal and cleaning products are presented in Table 2, Table S1, and Fig. 3. Estimations of mineral contents by optical microscopy indicate that raw coal is enriched in clay minerals with less quartz and other minor mineralogical components (carbonates and pyrite). The DMCs separation procedures employed at the preparation plant have different effects on the mineral matter. Clay minerals are efficiently removed and significantly enriched in the middlings and coal gangue, leaving only 1.7 vol.% total minerals in the cleaning coal sample. Note that the SiO_2/Al_2O_3 ratio of coal gangue (2.0) is higher than that of other samples and kaolinite (1.18), probably indicating quartz is easily partitioned into heavy fractions.

In detail, the distribution behavior of minerals during coal beneficiation is heavily dependent on the modes of occurrence of minerals. Based on the XRD data and SEM observation, the major minerals in waste products (in the decreasing order of significance) are kaolinite and quartz. Other minerals such as calcite, ankerite, pyrite, illite,

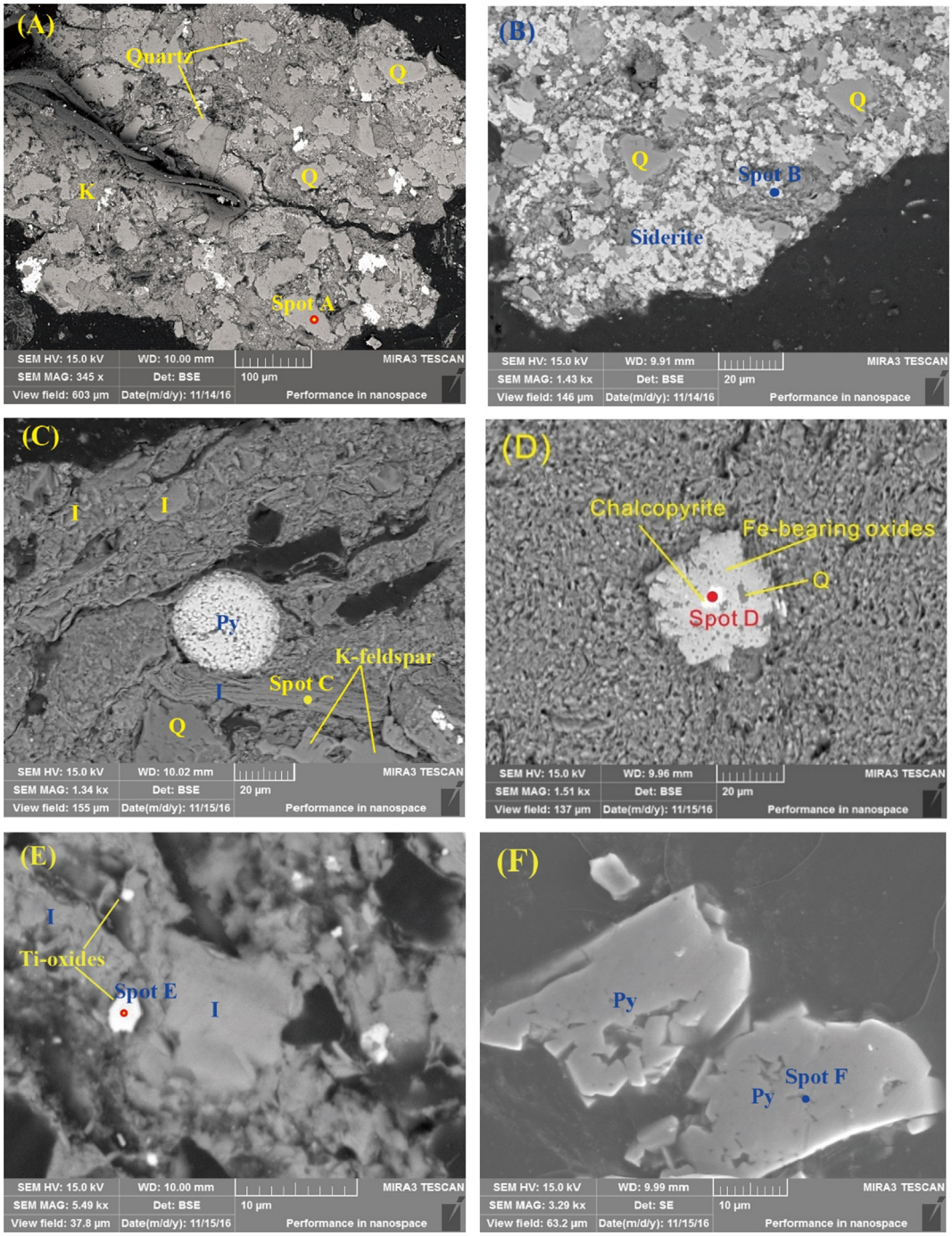

Fig. 3. Mineralogical characteristics of coal cleaning wastes detected by SEM-EDX techniques. (A) detrital quartz dispersed and mixed with clay minerals (kaolinite) in the middlings (BSE). (B) Massive siderite and quartz in the middlings (BSE). (C) Illite, K-feldspar, quartz, and spherical pyrite grain in coal gangue (BSE). (D) Chalcopyrite and iron-bearing oxides minerals in coal gangue (BSE). (E) Anatase/rutile and illite in coal slime (BSE). (F) Massive pyrite in coal slime (SE). K: kaolinite; I: illite; Q: quartz; Py: pyrite.

chalcopyrite, albite, K-feldspar, anatase/rutile, and magnetite are also identified as minor and accessory species. Clean coal is enriched in clay minerals such as kaolinite.

Clay minerals are widely distributed and dominated by kaolinite and with lesser amounts of illite. Clay mineral mainly occurs as massive lumps (Fig. 2A), bands (Fig. 2B), or irregular aggregates of fine-grained particles. In places, clay is the groundmass for the organic macerals and other minor minerals in the waste products (Fig. 2D). The modes of occurrence of clay are very different in the clean coal and mainly disseminated in the collodetrinite or collotellinite (Fig. 2B). There are also a few authigenic clays (kaolinite) found in the cell cavities of the coal macerals, and they sometimes occur as coatings on framboidal pyrite or contain inclusions of cleat-infillings calcite. The modes of occurrence of clay indicate that they may derive from multiple origins including detrital terrigenous origin (primary origin), authigenic/syn-depositional precipitation origin, and epigenetic origin. The cleaning circuits play an important role in shifting the clays of terrigenous origin from raw coal into the wastes products. Quartz occurs as angular grains and sometimes as particles with good abrasion occurring as rounded or subangular quartz grains (Fig. 3A), with particle sizes larger than 10 μm. The modes of occurrence of quartz suggest that it was mainly derived from terrigenous inputs, and the sediment-source region

(perhaps Yinshan uplift) for the Huaibei coal basin is far away and thus quartz may have been subjected to intensive transport to the peat [33,37]. Quartz is often mixed with clays in the preparation products and cannot be found in the clean coal; this is also consistent with the chemical ratio of SiO_2/Al_2O_3 (0.94) for clean coal. Carbonate minerals, including epigenetic calcite and dolomite/ankerite, are present as cleat infillings (Fig. 2C) in the waste products, whereas siderite occurring as nodules (Fig. 3B) is indicative of authigenic precipitation within the peat-forming environment [2,38]. Although the quantitative analysis for the carbonate mineral was not carried out, the chemical analysis results of major oxides suggest that the middlings are relatively enriched in carbonate minerals because of the higher content of CaO (1.18%) in middlings. Pyrite is an important carrier for many toxic elements in coal [1–10,39]. In spite of the low contents of inorganic sulfur, syngenetic framboidal pyrite can be observed in all the washed products (including clean coal), and sometimes epigenetic pyrite-infillings are found in middlings and coal gangue (Fig. 2D and F). It might be inferred from the results of sulfide-S and iron oxide content that pyrite is relatively enriched in coal gangue. Minor anatase/rutile and chalcopyrite, iron-bearing minerals can also be identified by the means of SEM-EDS techniques (Fig. 3D and 3E). Minerals that are relatively enriched in the waste products can be very important hosts for trace metals. Toxic elements such as As (Fig. S1e), Pb (Fig. S2), V (Fig. S1e), Cu (Fig. S1d and 1f), Co (Fig. S1b), and Mn (Fig. S1b) can be directly detected by energy dispersive X-ray spectroscopy. The information together with SCE results are critical to elucidating the modes of occurrences of toxic elements, and will help to explain their transformation behaviors during coal washing and/or combustion, as discussed in the following sections.

3.3. Distribution of major element oxides and trace elements

The content of major element oxides and trace elements is given in Table 3. Few reports have been made to evaluate the mass balance of trace elements for the samples from coal washing plants. Some researchers calculated the removal or enrichment ratio of trace element based on the laboratory float-sink experiment data [7]; and others calculated the elemental differences between each product and raw coal which then divided by the element concentrations in the raw coal to determine the removal/enrichment ratio for the preparation plant products [6,8–10]. We have tried to get the plant historical data of yields of various product streams to calculate the mass balance of the trace elements (Table 3). The mass balance ratio (R) is calculated as:

$$R(\%) = \frac{c_m * y_m + c_c * y_c + c_s * y_s + c_g * y_g}{c_r * y_r} \times 100\%$$

c_r, c_m, c_c, and c_g represent the element contents for raw coal, middlings, clean coal, slime and coal gangue, respectively; y_r, y_m, y_c, y_s and y_g represent the yield of raw coal, middlings, clean coal, coal slime, and gangue, respectively. Based on the data provided from Luling preparation plant, the yield of middlings, clean coal, slime, and coal gangue are 5.22%, 58.3%, 6% and 31.02%, respectively. As shown in the table, the mass balance ratio ranges from 51% to 179% for trace elements and 72% to 339% for the major element oxides, respectively. Of these elements, major element oxides including Na_2O (339%), P_2O_5 (302%), Fe_2O_3 (183%), and SiO_2 (141%), and trace elements including Cr (51%) and Pb (179%) are not in the acceptable range considering that the value of the balances reported in some publications with regard to power plant is within the range of 70–130% [28,62]. However, the process in preparation plant is different from power plant. Many variations and factors during the industrial coal preparation process in this study as mentioned in Part 2.1 can cause errors for evaluating the mass balance for the trace elements. The content of elements in the composite raw coal is dynamic but within the range of the run-of-mine coal from Luling coal seams 8, 9 and 10 (unpublished data). In addition, the contents of major element oxides such as Fe_2O_3 are higher in the output products, possibly because of the medium such as magnetite contained in the beneficiation products that cannot be completely separated by the magnetic separator (Fig. S3).

3.4. Transformation behavior of toxic elements during coal washing

The concentration and SCE results of toxic trace elements in the raw coal and preparation plant wastes are presented in Table 3, Table 4, and Fig. 4, respectively. The total leaching ratio of SCE ranges from 71.1% to 115.7%, except for cobalt in raw coal (65.8%). The recovery of sequential extraction experiments can be acceptable within 70% to 130% [28,30,32,48,51]. Sequential extraction procedure has been widely used but has some limitations. A complete extraction of a component is not readily achieved in any stage of sequential leaching experiments. During the SCE process, the mass loss or contamination seems inevitable because many regents and several steps are involved. Therefore, the direct method (SEM-EDS) was adopted in this study to overcome the problem.

The partitioning behavior of V and Cr between different separations will be discussed together because of their similar geochemical properties and transformation behavior during the coal washing process [1,30]. Approximately 40% of V and 83% of Cr are efficiently removed from the raw coal, and the remainder is concentrated in the coal wastes products. As shown in Fig. 4, silicates and organic matters are the primary associations for V and Cr in the raw coal and waste products, which is also confirmed by the SEM-EDS analysis (Figs. 3E and S1e). Compared to coal gangue, the proportions of organic-bound V and Cr are relatively higher in the middlings (25.3% for V; 49.7% for Cr) and coal slime (30.4% for V; 37.0% for Cr) samples. Similarly, Huggins et al. [1,40,42] investigated inorganic-rich sink fractions and tailings, suggesting that illite could be the hosts for V and Cr in coal. Zhao et al. [41] found that V and Cr were enriched in nano Ti-oxides mineral grains that were formed by authigenic precipitation and contained within coal macerals or pores.

Although the sequential extraction results show that Cu, Cd, As, and Zn have multiple chemical forms, they are mainly associated with sulfides in the waste products. It has been established that sulfides minerals, such as pyrite, sphalerite, galena, and chalcopyrite in the coal are the primary carriers for these elements [39]. The observation under SEM-EDS also shows that Cu occurs in chalcopyrite in coal gangue or in pyrite in the coal slime (Fig. 3D and F). The slight enrichment of Cu in the wastes might be a reflection of sulfides reporting to the waste streams rather than the washed coal (Table 3). The modes of occurrence of As, Cd, and Zn are primarily associated with sulfide minerals in raw coal (Fig. 4). Arsenic and Cd are efficiently partitioned from the raw coal to coal gangue, leaving the latter with the highest concentrations (Table 3). The fractions of sulfide-bound elements Cd, As, and Zn in coal gangue are higher than in coal slime and middlings, which may be ascribed to higher contents of sulfides in the gangue sample.

The distribution of Se between raw coal and beneficiation products suggests that Se might have a strong affinity with organic matter in the raw coal (Table 3). Further, Se is consistently associated with organic matters (57.1%) and silicates (24.5%) in the raw coal (Fig. 4). After coal beneficiation, the fractionation profile of Se speciation for the middlings and coal slime is similar to that of the raw coal where the organic-bound Se is dominant; whereas the coal gangue contains the lowest organic associations of Se (15.6%). Se is considered to be associated with sulfide minerals or some accessory minerals in coal [4,44–46]. It is also well-documented that Se could be found in greater abundance as organically-associated form [44–48]. The modes of occurrence of Pb are equally comprised of organic-bound and silicate-bound (each around 30%) associations, followed by carbonate-bound (20.4%) and sulfide-bound (19.3%) associations in the raw coal (Fig. 4). Sequential extraction experiments suggested that the carbonate-associated fraction (48.2%) and organically-bound fraction (28.3%) are the

Table 3
The contents of major element oxides and trace elements as well as element mass balance for the Luling preparation plant samples.

	Raw coal	Midlings	Clean coal	Coal slime	Gangue	Output	R (%)
SiO_2	15.14	24.14	5.09	21.06	51.13		
Mass (%)	3.575	0.298	0.701	0.298	3.745	5.04	141.03%
TiO_2	0.41	0.57	0.22	0.05	0.88		
Mass (%)	0.097	0.007	0.030	0.001	0.064	0.10	105.85%
Al_2O_3	9.53	13.7	5.42	13.61	25.51		
Mass (%)	2.250	0.169	0.746	0.193	1.868	2.98	132.26%
Fe_2O_3	0.67	2.03	0.14	1.3	3.1		
Mass (%)	0.158	0.025	0.019	0.018	0.227	0.29	183.17%
MgO	0.82	0.94	0.63	0.79	1.16		
Mass (%)	0.056	0.003	0.032	0.003	0.017	0.06	100.54%
CaO	0.61	1.18	0.35	0.66	0.44		
Mass (%)	0.144	0.015	0.048	0.009	0.032	0.10	72.42%
MgO	0.82	0.94	0.63	0.79	1.16		
Mass (%)	0.194	0.010	0.113	0.012	0.060	0.19	100.54%
MnO	0.052	0.05	0.05	0.05	0.06		
Mass (%)	0.012	0.001	0.007	0.001	0.004	0.01	102.64%
Na_2O	0.23	0.1	0.2	0.18	0.3		
Mass (%)	0.054	0.024	0.047	0.042	0.071	0.18	339.13%
K_2O	0.52	0.45	0.28	0.56	1.1		
Mass (%)	0.123	0.005546	0.038541	0.007933	0.080562	0.13	107.99%
P_2O_5	0.04	0.02	0.03	0.05	0.32		
Mass (%)	0.009	0.000	0.004	0.001	0.023	0.03	302.00%
V (mg/kg)	70	38	43	40.5	115		
Mass (mg)	70	1.98	25.07	2.43	35.67	65.16	93.08%
Cr (mg/kg)	30	24.5	5.04	18.4	31.85		
Mass (mg)	30	1.28	2.94	1.1	9.88	15.2	50.67%
Co (mg/kg)	5.12	5.44	3.79	3.21	7.6		
Mass (mg)	5.12	0.28	2.21	0.19	2.36	5.04	98.51%
Ni (mg/kg)	11.66	11.42	8.51	8.14	15.13		
Mass (mg)	11.66	0.6	4.96	0.49	4.69	10.74	92.1%
Cu (mg/kg)	30.08	46.64	32.82	42.04	42.46		
Mass (mg)	30.08	2.43	19.13	2.52	13.17	37.26	123.88%
Zn (mg/kg)	49.47	59.61	44.58	71.3	94.16		
Mass (mg)	49.47	3.11	25.99	4.28	29.21	62.59	126.52%
Pb (mg/kg)	11.02	37.44	14.04	22.77	26.43		
Mass (mg)	11.02	1.95	8.19	1.37	8.2	19.7	178.81%
As (mg/kg)	3.61	4.98	0.77	3.32	8.35		
Mass (mg)	3.61	0.26	0.45	0.2	2.59	3.5	96.9%
Se (mg/kg)	4.27	5.04	4.3	4.58	3.03		
Mass (mg)	4.27	0.26	2.51	0.27	0.94	3.98	93.32%
Sn (mg/kg)	4.17	3.79	3.35	2.71	4.26		
Mass (mg)	4.17	0.2	1.95	0.16	1.32	3.63	87.17%
Sb (mg/kg)	0.61	0.5	0.47	0.64	0.82		
Mass (mg)	0.61	0.03	0.27	0.04	0.25	0.59	97.19%
Cd (mg/kg)	0.33	0.33	0.25	0.36	0.59		
Mass (mg)	0.33	0.02	0.15	0.02	0.18	0.37	111.39%

R: mass balance ratio; The unit for major element oxides is % and for other elements is mg/kg.

dominated forms in the middlings. The mineralogical components shown in Tables 3 and S2 as well as observation by SEM-EDS show that carbonate minerals are relatively enriched in middlings, and subsequently caused the enrichment of some carbonate-bearing elements such as Mn, Pb, and Co in the middlings. In addition, silicate-bound Pb is the predominant form in the coal slime and gangue samples.

The Sb content in the samples is in the range of 0.47–0.82 μg/g, which is lower than the average content of Sb in Chinese coals [37] and world coals [49]. The solid wastes have a relatively higher Sb content while the clean coal is low in Sb, suggesting an inorganic affinity of Sb in the coal. Based on the SCE results, silicate-bound Sb is most abundant in raw coal and waste product (Fig. 4). Generally, an increase in the silicate-bound form and a decrease in the organic- bound Sb have been observed (Fig. 4). It is generally accepted that Sb in coal is associated with sulfides [43,50]. In this study, the result of SEM-EDS analysis on the samples suggests that clay minerals, such as illite, could be the major hosts for Sb (Figs. 3C and S1c). Sb occurrence in clay minerals in coal have been reported by some researchers [51–54]

The content of Co is similar in the raw coal and in the middlings, and it is concentrated in coal gangue while depleted in the clean coal. Multiple modes of occurrence of Co may be present in the raw coal and it is probably associated with sulfide minerals, silicates, and organic matters [46,55]. Based on the SCE results, Co mainly occurs as silicates (40.5%) and carbonates (38.6%) in the raw coal (Fig. 4). Ward et al. [55] found that Co exhibited a significant correlation with Fe (especially strong for siderite), indicating Co in the coal might be associated with siderite. This is also similarly supported by our SEM-EDS technique that siderite ($FeCO_3$) contains minor Co as impurities in siderite crystals (Figs. 3B and S1c). After coal washing, the fractions of carbonate-bound Co are increased in the middlings (44.2%) and show small differences between raw coal and the other waste products.

As indicated in Fig. 4, the modes of occurrence of Ni in the raw coal are dominated by sulfide minerals (35.3% for Ni) and followed by the silicates-bound (28.3%) and organic-bound (21.8%) associations. Nickel is geochemically similar to Fe and could substitute for Fe in the pyrite [39,45]. Some researchers have reported that Ni in coals might be organically bound [45] or associated with sulfide minerals [39,45–46]. It was also found that Ni could be associated with clays, oxides, and hydroxides minerals [56]. The total fractions of sulfide-bound Ni and silicate-bound Ni in raw coal is up to 63.6% and are

Table 4
Results of sequential chemical extraction for 11 toxic elements in raw coal and solid wastes.

Elements	V (μg/g)	Cr (μg/g)	Co (μg/g)	Ni (μg/g)	Cu (μg/g)	Cd (μg/g)	As (μg/g)	Se (μg/g)	Sb (μg/g)	Pb (μg/g)	Zn (μg/g)
Raw coal											
Water-leachable	bdl	bdl	bdl	bdl	bdl	0.00	bdl	0.02	0.05	bdl	bdl
Ion-exchangeble	bdl	0.02	0.12	0.45	0.55	0.01	0.05	0.26	0.03	bdl	bdl
Carbonate-bound	1.51	1.49	1.29	1.52	0.98	0.03	0.09	2.31	0.02	1.99	6.73
Organic-bound	16.40	10.39	0.36	2.94	15.74	0.06	0.47	0.44	0.15	2.94	10.91
Slicate-bound	28.82	16.72	1.36	3.81	6.25	0.05	0.74	0.99	0.29	2.94	7.27
Sulfide-bound	3.06	2.31	0.22	4.76	9.20	0.11	1.63	0.02	0.09	1.88	22.28
Sum	49.79	30.92	3.35	13.48	32.71	0.27	2.97	4.04	0.64	9.75	47.20
Bulk analysis	70.00	30.00	5.12	11.66	30.08	0.33	3.61	4.27	0.61	11.02	49.47
Mass balance (%)	71.12%	103.08%	65.38%	115.70%	108.74%	82.23%	82.38%	94.07%	104.20%	88.48%	95.40%
Middlings											
Water-leachable	0.00	0.02	0.01	0.01	bdl	bdl	0.03	bdl	0.08	0.01	bdl
Ion-exchangeable	0.07	0.39	0.28	0.64	0.87	0.01	0.00	0.05	0.00	0.03	0.57
Carbonate-bound	2.24	1.27	2.56	0.64	0.13	0.03	0.12	0.04	0.03	16.31	20.81
Organic-bound	8.51	13.05	0.50	1.51	9.47	0.09	1.27	2.20	0.11	9.56	6.08
Slicate-bound	19.86	10.78	1.46	3.78	15.72	0.06	1.05	1.23	0.27	7.12	16.66
Sulfide-bound	2.92	0.75	0.98	4.16	22.72	0.11	1.73	0.69	0.03	0.77	22.93
Sum	33.61	26.26	5.79	10.74	48.91	0.29	4.20	4.20	0.51	33.79	67.04
Bulk analysis	38.00	24.50	5.44	11.42	46.64	0.33	4.98	5.04	0.50	37.44	59.61
Mass balance (%)	88.43%	107.19%	106.45%	94.08%	104.86%	87.35%	84.31%	83.43%	102.23%	90.21%	112.47%
Coal slime											
Water-leachable	0.15	0.02	0.20	bdl	0.01	bdl	0.00	0.00	0.11	0.02	0.00
Ion-exchangeble	0.12	0.39	0.17	0.59	0.66	0.01	0.00	bdl	0.01	0.02	0.34
Carbonate-bound	2.82	bdl	0.41	bdl	0.01	0.02	0.15	0.21	0.01	5.11	10.59
Organic-bound	10.25	5.74	0.62	2.76	13.34	0.11	0.93	2.51	0.18	4.17	7.77
Slicate-bound	18.42	9.35	0.88	3.40	14.08	0.07	0.52	0.78	0.25	10.05	18.90
Sulfide-bound	1.93	bdl	0.16	2.12	13.08	0.15	1.36	0.64	0.05	1.70	35.45
Sum of six forms	33.68	15.49	2.44	8.88	41.18	0.35	2.96	4.14	0.60	21.07	73.05
Bulk analysis	40.50	18.59	3.34	8.14	42.04	0.36	3.32	4.58	0.64	22.77	71.30
Mass balance (%)	83.15%	84.21%	72.93%	109.06%	97.95%	97.91%	89.28%	90.48%	93.75%	92.53%	102.45%
Coal gangue											
Water-leachable	0.01	0.02	bdl	bdl	0.00	0.00	bdl	0.04	0.10	0.00	0.02
Ion-exchangeble	0.09	0.40	0.62	0.98	0.87	0.01	0.00	0.20	0.00	0.03	0.42
Carbonate-bound	2.84	3.14	3.06	bdl	4.62	0.06	0.77	0.14	0.03	6.87	12.18
Organic-bound	14.77	3.77	0.64	2.20	10.20	0.04	0.91	0.41	0.09	2.46	21.40
Slicate-bound	64.05	20.44	2.52	4.27	4.24	0.10	2.01	1.20	0.52	11.57	18.89
Sulfide-bound	6.82	2.69	1.10	6.47	20.52	0.42	4.37	0.66	0.01	0.30	36.11
Sum of six forms	88.57	30.46	7.93	13.92	40.46	0.63	8.06	2.65	0.77	21.23	89.01
Bulk analysis	115.00	31.85	7.60	15.13	42.46	0.59	8.35	3.03	0.82	26.43	94.16
Mass balance (%)	77.02%	95.64%	104.34%	92.02%	95.28%	106.78%	96.54%	87.57%	93.44%	80.34%	94.53%

bdl: below detection limit.
Sum: sum of six form element concentrations.
Bulk analysis: elements determined in bulk samples.
Mass balance (%): data of the sum of six forms divided by bulk analysis result.

similar with coal slime (62.2%), but lower than in the middlings (73.9%) and coal gangue (77.2%), and these two forms might cause the lower contents of Ni in the cleaning coal and slime.

3.5. Thermochemical and toxic elements behavior during combustion

3.5.1. Thermal reactivity during combustion

The thermogravimetric analysis could provide important information regarding the reactivity and transformation behaviors of fuels during combustion. The TG-DTG curves of raw coal and corresponding beneficiation products at the heating rate of 15 °C/min were plotted in Fig. 5. Meanwhile, the characteristic of TGA parameters determined from the combustion profiles were summarized in Table 5.

Overall, as shown in Fig. 5, the raw coal and beneficiation products (except for coal gangue) exhibit a similar trend when the combustion temperature increased. At the initial stage, the weight loss between 40 °C and 140 °Cis mainly because of dehydration of moisture in the samples. There is a net weight gain from 195 to 357 °C corresponding to the oxygen chemisorption before the onset of combustion. A similar phenomenon was also found in our previous investigations on bituminous coal and coal gangue combustion [22,57]. The devolatilization process is inconspicuous for all the samples and no single peak was found in the combustion profiles due to the relatively higher coal rank. There is one typical sharp peak in the temperature range of 310–620 °C for all samples (except for coal gangue) resulted from thermal decomposition of the samples including devolatilization, charring, and combustion of volatiles and char.

For each beneficiation products, the maximum weight loss rate (R_{max}) exhibits the following decreasing order: clean coal (0.87%/°C) > coal slime (0.62%/°C) > middlings (0.49%/°C) > coal gangue (0.11%/°C), while the corresponding temperature T_{max} exhibits insignificant differences and displays as following order: clean coal (472.4 °C) < middlings (480.8 °C) < coal slime (484.4 °C) < coal gangue (486.3 °C). Compared to raw coal, it is evident that the DMCs process greatly improves the reactivity of raw coal, producing clean coal with an increase of 22.5% in the reactivity parameters R_{max}. This is consistent with the higher proportions of vitrinite, liptinite, and volatile matters in the cleaning coal. The solid waste products, middlings, and coal slime are also not difficult to burn in the boilers because the onset temperature and reactivity parameters during combustion are similar to the raw coal as suggested from Fig. 5 and Table 5. In contrast to middlings and coal slime, the gangue sample with high ash yield is difficult to burn as indicated by the TG-DTG combustion profiles (Fig. 5). The R_{max} for coal gangue decreases by 0.11%/°C (equal to 84.51%), while

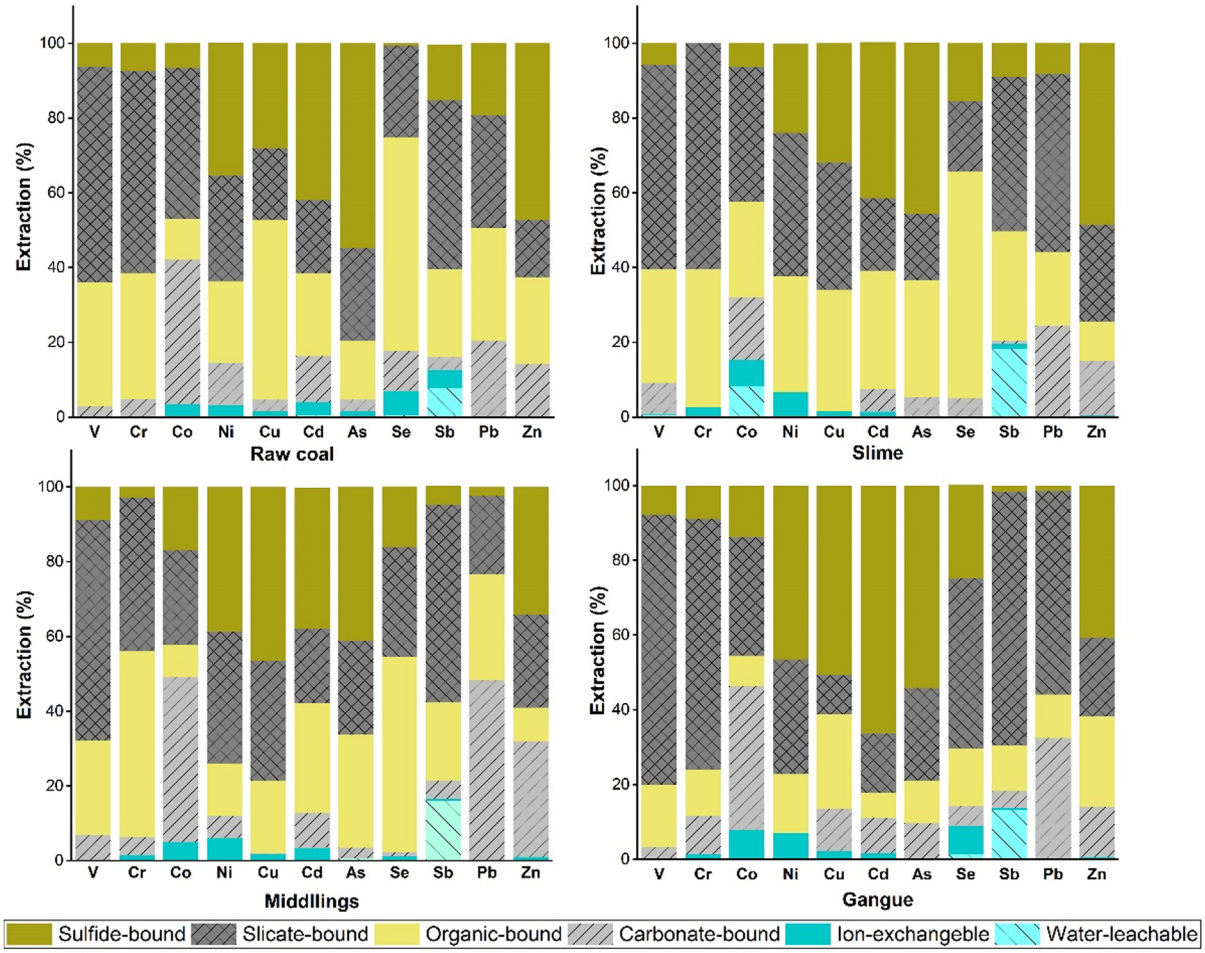

Fig. 4. Comparisons of chemical forms of 11 toxic elements in raw coal and its waste products.

an 11.5 °C increase of the corresponding T_{max} is observed. There is a broader main peak presented in the DTG profile of coal gangue (Fig. 5). The high ash content of gangue inhibits the thermal decomposition of the organic matter during combustion. In addition, clay minerals (kaolinite) as the major components may also contribute to the weight loss of the sample since kaolinite will lose structural OH at around 500 °C[57].

3.5.2. Volatility of toxic elements in coal preparation plant waste products

It has been experimentally found that many toxic elements will volatilize during combustion, and the fates of trace elements are determined by the modes of occurrences, physiochemical reactions, operating conditions, etc. [23–26,57–68]. Trace elements associated with organic matter or sulfide minerals are easily vaporized during the early stage of coal combustion. Elements occurring as excluded minerals or discrete minerals are more likely to be concentrated in ash whereas

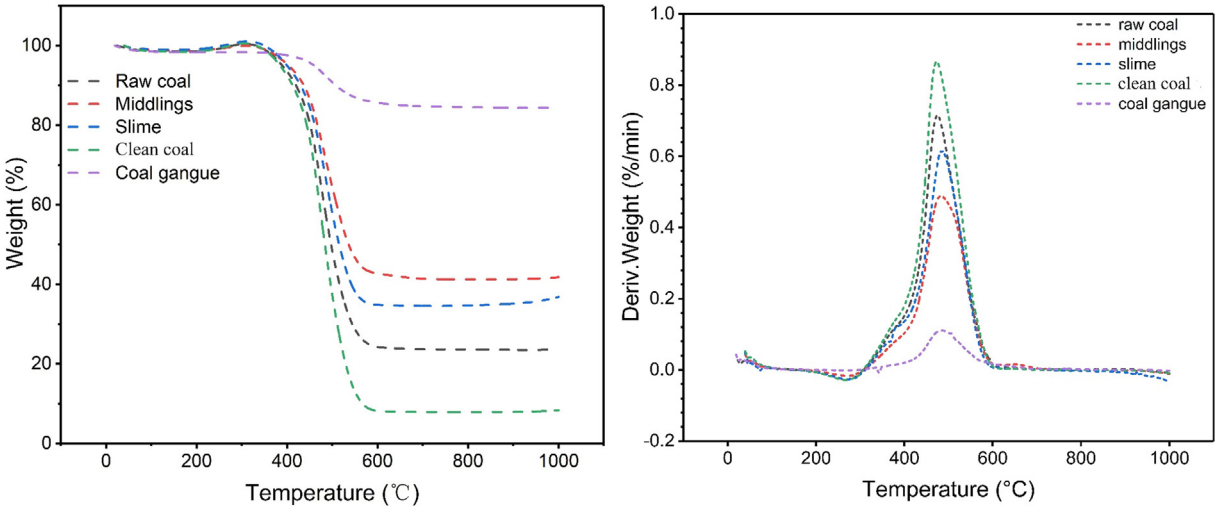

Fig. 5. TG-DTG curves of raw coal and beneficiation products during combustion under air flow.

Table 5
DTG data of raw coal and cleaning products at the heating rate of °C/min.

Sample	T_{max}(°C)	R_{max}(%/°C)	R_{max}change [a] (%)	T_{max}change [a] (%)
Raw coal	474.8	0.71		
Middlings	480.8	0.49	−30.98	1.27
Coal slime	484.4	0.62	−12.67	2.02
Clean coal	472.4	0.87	22.54	−0.52
Coal gangue	486.3	0.11	−84.51	2.42

R_{max}: the maximum rate of weight loss.
T_{max}: the peak temperature when weight loss rate is maximum.
[a] Change: positive sign indicates an increase, while a negative sign means a decrease toward raw coal.

elements associated with inherent minerals or chemically bound to the organic compounds preferentially form submicron particles [61,62]. To assess the volatile characteristics of toxic elements during combustion, the volatile ratio (Vr) was calculated using the formula as following [57]

$$Vr\% = \left[1 - \frac{\text{Concentration of element in ash} \times \text{Ash yield in the corresponding sample}}{\text{Concentration of element in the corresponding sample}}\right] \times 100\%$$

As indicated from Fig. 6, the toxic elements can be classified into three distinct groups based on their volatile characteristics. Group 1 includes the highly volatile elements Se with Vr > 85%. Selenium in the studied samples mainly occur in organic matter, as mentioned above. During the devolatilization stage and char combustion, the structure of organic matter will be destroyed and the organic-bound inorganics could be released and vaporized. Many studies have also reported that Se is easily vaporized and released with flue gas phase into the atmosphere or condensed onto the fine particles and absorbed by it physically and chemically [26,61,64].

Group 2 contains elements As, Pb, Zn, Cd, and Sb, with the Vr in the range of 20–85%. The volatile ratio of As varies among the samples (44–77%). Previous studies reported that pyritic-As vaporized with the decomposition of pyrite to pyrrhotite or with oxidation of arsenopyrite to ferric arsenate [23]; meanwhile, the organically bonded arsenic possibly transformed to arsenic oxide [23]. In the present study, sulfide- and organic-bound arsenic are the dominant forms for all of the fractions which result in about 70% of arsenic volatized during combustion. For the gangue sample, the volatile ratio is relatively lower (44.5%). Arsenic in the coal gangue is primarily associated with sulfide minerals and then with silicates. High contents of iron oxides, silicon oxides, and aluminum oxides in the high temperature ash of coal gangue might play

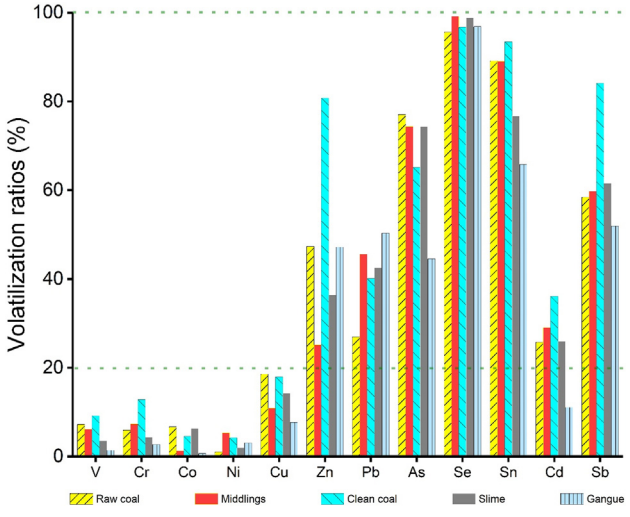

Fig. 6. The volatile ratio of toxic trace elements in raw coal and associated cleaning products.

an important role in capturing As to form stable phases, such as Fe oxides, hydroxides, sulfates, arsenate [23,64–66], or as an As-bearing aluminosilicate glass phase in the ash [65]. Other elements, such as Sb, Cd, Zn, and Pb in the second group have volatile ratio in the range of 11.1–36.1%, 51.9–84.1%,25.2–80.8%, and 26.9–50.3%, respectively; of these elements, the volatile ratio of Sb, Cd, and Zn increased to the maximum in the clean coal sample, while Pb exhibit the maximum mass loss in the coal gangue. The maximum vaporization of Sb, Cd and Zn in the cleaning coal during combustion might be associated with their organically associations after heavy medium separation.

The least volatile elements V, Cr, Co, Ni, and Cu with Vr less than 20% are placed into Group 3. The volatile degrees of V, Cr, Co, and Ni are lower, having volatile ratio in the range of 1.4–7.2% (V), 4.3–12.8% (Cr), 0.7–6.7% (Co), and 1.0–5.4% (Ni). Although these elements partly occur as organic or sulfide associations in the samples, few of them are driven off with the escape of organic matter. In a laboratory coal combustion experiments, Wang et al. [23] found that V, Cr, Co, and Ni exhibited no or very low volatility in spite of the combustion conditions and heating rates. Other combustion experiments under air condition or oxy-combustion condition confirmed that V, Cr, Co and Ni were of low volatility [30,59,67]. Further, it also has been demonstrated by thermodynamic equilibrium calculation or investigation on the combustion ash from power plant that the V, Cr, and Co were hardly vaporized [26,68]. The low volatility of V, Cr, Co and Ni in this study may be associated with their chemical speciation. Elements bound with silicate minerals, such as illite, are more likely to remain in the ash [24]. The volatile ratio of V, Cr, and Co in the raw coal are significantly raised in the clean coal while decreased in the coal gangue sample (Fig. 6). In contrast, the volatile behavior of Cu is slightly different from V, Cr, Co, and Ni. The volatile ratio of Cu is lower in the waste products (7.7–14.2%) than that in raw coal (18.6%) and clean coal (17.9%). Querol et al. [59] found that Fe-bearing phases segregated into slag during coal combustion, leading to the enrichment of Cu, Fe, and Mn with iron oxide affinity. As indicated in Section 4, Cu occurs mainly as chalcopyrite, pyrite, and silicates in the wastes sample, and bound with organic matters and sulfides in the raw coal. Affinities with iron sulfides and discrete minerals result in lower volatility of Cu in the waste products; whereas dominant organic associations of Cu might be one of the most important factors to explain the relatively higher volatile ratio for the raw coal and clean coal.

4. Conclusions

A comprehensive study of the petrology, mineralogy and geochemistry of beneficiation products from DMCs process in a coal cleaning plant was carried out. The preparation plant wastes derived from the three-product DMCs exhibits enrichment of mineral matter to different degrees. Mineral forms such as massive lumps of clays of terrigenous origin, cleat-infilling carbonate, and pyrite of epigenetic origin are prone to be enriched in the middlings and coal gangue. Detected minor or trace heavy minerals, quartz, rutile/anatase, and chalcopyrite also likely reported to the preparation plant wastes. The contents of low-density density vitrinite and liptinite were enhanced in the clean coal, while inertinite-maceral group were enriched in the middlings. The modes of occurrences of the elements varied among different coal waste products, and the transformation behavior of toxic elements between the raw coal and the washery products were mainly controlled by clay minerals (V, Cr, Co, Sb, and Pb), carbonate minerals (Co and Pb), sulfide minerals (As, Cu, Ni, Cd, and Zn) and organic matters (V, Cr, Se, and Cu). The thermal reactivity of coal is significantly improved after coal beneficiation, whereas the increased inorganic components inhibit the thermal chemical reaction of wastes (especially for coal gangue). Three groups are divided based on the volatile ratio of elements. The organic-mineral associations of toxic elements make significant contributions to the transformation behavior during combustion.

Acknowledgments

This work was supported by the National Natural Science Foundation of China (41672144), the Nature Science research project of Anhui Province, China (1408085MB29), the Research Projects of Department of Land and Resources of Anhui Province, China (2016-K-2), and the National Key R&D Program of China (2016YFC0201600). Biao Fu thanked Chinese Scholarship Council for his joint-PhD scholarship studying at the University of Kentucky. We acknowledge editors and reviewers for polishing the language of the paper and for in-depth discussion.

Appendix A. Supplementary data

Supplementary data associated with this article can be found, in the online version, at http://dx.doi.org/10.1016/j.fuel.2018.04.085.

References

[1] Huggins FE, Seidu LBA, Shah N, Huffman GP, Honaker RQ, Kyger JR, et al. Elemental modes of occurrence in an Illinois #6 coal and fractions prepared by physical separation techniques at a coal preparation plant. Int J Coal Geol 2009;78(1):65–76.
[2] Ward CR. Analysis, origin and significance of mineral matter in coal: an updated review. Int J Coal Geol 2016;165:1–27.
[3] Diehl SF, Goldhaber MB, Koenig AE, Lowers HA, Ruppert LF. Distribution of arsenic, selenium, and other trace elements in high pyrite Appalachian coals: evidence for multiple episodes of pyrite formation. Int J Coal Geol 2012;94(94):238–49.
[4] Hower JC, Robertson JD. Clausthalite in coal. Int J Coal Geol 2003;53(4):219–25.
[5] Dai S, Zeng R, Sun Y. Enrichment of arsenic, antimony, mercury, and thallium in a Late Permian anthracite from Xingren, Guizhou, Southwest China. Int J Coal Geol 2006;66(3):217–26.
[6] Akers D, Dospoy R. Role of coal cleaning in control of air toxics. Fuel Process Technol 1994;39(1):73–86.
[7] Bergh JP, Falcon RMS, Falcon LM. Trace element concentration reduction by beneficiation of Witbank Coalfield no. 4 Seam. Fuel Process Technol 2011;92(4):812–6.
[8] Vassilev SV, Eskenazy GM, Vassileva CG. Behaviour of elements and minerals during preparation and combustion of the Pernik coal, Bulgaria. Fuel Process Technol 2001;72(2):103–29.
[9] Wang W, Qin Y, Sang S, Jiang B, Guo Y, Zhu Y, et al. Partitioning of minerals and elements during preparation of Taixi coal, China. Fuel 2006;85(1):57–67.
[10] Yossifova MG. Petrography, mineralogy and geochemistry of Balkan coals and their waste products. Int J Coal Geol 2014;122(Supplement C):1–20.
[11] Zou W, Cao Y, Zhang Z, Liu J. Coal petrology characteristics of middlings from Qianjiaying fat coal mine. Int J Min Sci Technol 2013;23(5):777–82.
[12] Fan P-p, Fan M-q, Liu A. Using an axial electromagnetic field to improve the separation density of a dense medium cyclone. Miner Eng 2015;72(Supplement C):87–93.
[13] Dou D, Yang J, Liu J, Zhang H. A novel distribution rate predicting method of dense medium cyclone in the Taixi coal preparation plant. Int J Miner Process 2015;142(Supplement C):51–5.
[14] Cutruneo CMNL, Oliveira MLS, Ward CR, Hower JC, Brum IASD, Sampaio CH, et al. A mineralogical and geochemical study of three Brazilian coal cleaning rejects: demonstration of electron beam applications. Int J Coal Geol 2014;130:33–52.
[15] Haibin L, Zhenling L. Recycling utilization patterns of coal mining waste in China. Resour Conserv Recycl 2010;54(12):1331–40.
[16] Bian Z, Miao X, Lei S, Chen SE, Wang W, Struthers S. The challenges of reusing mining and mineral-processing wastes. Science 2012;337(6095):702.
[17] Duffy GJ, Lanauze RD, Kable JW. Reducing the environmental impact of coal-washing practice in Australia. Miner Environ 1981;3(4):103–10.
[18] La Nauze RD, Duffy GJ. Coal rejects — a wasted resource? Environ Geochem Health 1985;7(2):69–79.
[19] Kavidass S, Bakshi VK, Diwakar KK. Overview and status of first 25 MW (e) IR-CFB boiler in India. New York, NY (United States): American Society of Mechanical Engineers; 1997.
[20] Liu X. The application of and prospects for fluidized-bed combustion technology in coal-mining areas in China. Energy 1986;11(11):1209–14.
[21] Biswas S, Choudhury N, Sarkar P, Mukherjee A, Sahu SG, Boral P, et al. Studies on the combustion behaviour of blends of Indian coals by TGA and drop tube furnace. Fuel Process Technol 2006;87(3):191–9.
[22] Zhou C, Liu G, Wang X, Qi C. Co-combustion of bituminous coal and biomass fuel blends: thermochemical characterization, potential utilization and environmental advantage. Bioresour Technol 2016;218:418.
[23] Wang J, Tomita A. A chemistry on the volatility of some trace elements during coal combustion and pyrolysis. Energy Fuels 2003;17(4):954–60.
[24] Xu M, Yan R, Zheng C, Qiao Y, Han J, Sheng C. Status of trace element emission in a coal combustion process: a review. Fuel Process Technol 2004;85(2):215–37.
[25] Méndez LB, Borrego AG, Martinez-Tarazona MR, Menéndez R. Influence of petrographic and mineral matter composition of coal particles on their combustion reactivity☆. Fuel 2003;82(15):1875–82.
[26] Yan R, Gauthier D, Flamant G. Volatility and chemistry of trace elements in a coal combustor. Fuel 2001;80(15):2217–26.
[27] Zhang L, Xia X, Zhang J. Improving energy efficiency of cyclone circuits in coal beneficiation plants by pump-storage systems. Appl Energy 2014;119:306–13.
[28] Zhou C, Liu G, Fang T, Wu D, Lam PKS. Partitioning and transformation behavior of toxic elements during circulated fluidized bed combustion of coal gangue. Fuel 2014;135:1–8.
[29] Zhou C, Liu G, Cheng S, Fang T, Lam PK. The environmental geochemistry of trace elements and naturally radionuclides in a coal gangue brick-making plant. Sci Rep 2014;4:6221.
[30] Liu Y, Liu G, Qi C, Cheng S, Sun R. Chemical speciation and combustion behavior of chromium (Cr) and vanadium (V) in coals. Fuel 2016;184(Supplement C):42–9.
[31] Dai S, Zou J, Jiang Y, Ward CR, Wang X, Li T, et al. Mineralogical and geochemical compositions of the Pennsylvanian coal in the Adaohai Mine, Daqingshan Coalfield, Inner Mongolia, China: modes of occurrence and origin of diaspore, gorceixite, and ammonian illite. Int J Coal Geol 2012;94(5):250–70.
[32] Dai S, Li D, Ren D, Tang Y, Shao L, Song H. Geochemistry of the late Permian No. 30 coal seam, Zhijin Coalfield of Southwest China: influence of a siliceous low-temperature hydrothermal fluid. Appl Geochem 2004;19(8):1315–30.
[33] Liu G, Vassilev SV, Gao L, Zheng L, Peng Z. Mineral and chemical composition and some trace element contents in coals and coal ashes from Huaibei coal field, China. Energy Convers Manage 2005;46(13):2001–9.
[34] Zheng L, Liu G, Wang L, Chou C-L. Composition and quality of coals in the Huaibei Coalfield, Anhui, China. J Geochem Explor 2008;97(2):59–68.
[35] Hower JC, Trinkle EJ, Wild GD. Maceral partitioning through beneficiation of Illinois Basin Coals. Coal Prep 1986;2(3):149–64.
[36] Wang W, Qin Y, Wei C, Li Z, Guo Y, Zhu Y. Partitioning of elements and macerals during preparation of Antaibao coal. Int J Coal Geol 2006;68(3):223–32.
[37] Dai S, Ren D, Chou CL, Finkelman RB, Seredin VV, Zhou Y. Geochemistry of trace elements in Chinese coals: a review of abundances, genetic types, impacts on human health, and industrial utilization. Int J Coal Geol 2012;94(3):3–21.
[38] Kortenski J. Carbonate minerals in Bulgarian coals with different degrees of coalification. Int J Coal Geol 1992;20(3):225–42.
[39] Kolker A. Minor element distribution in iron disulfides in coal: a geochemical review. Int J Coal Geol 2012;94(Supplement C):32–43.
[40] Huggins FE, Srikantapura S, Parekh BK, Blanchard L, Robertson JD. XANES spectroscopic characterization of selected elements in deep-cleaned fractions of Kentucky No. 9 Coal. Energy Fuels 1997;11(3):691–701.
[41] Zhao Y, Zeng F, Liang H, Tang Y, Li M, Xiang J, et al. Chromium and vanadium bearing nanominerals and ultra-fine particles in a super-high-organic-sulfur coal from Ganhe coalmine, Yanshan Coalfield, Yunnan, China. Fuel 2017;203(Supplement C):832–42.
[42] Seredin VV, Dai S, Sun Y, Chekryzhov IY. Coal deposits as promising sources of rare metals for alternative power and energy-efficient technologies. Appl Geochem 2013;31:1–11.
[43] Dai S, Yang J, Ward CR, Hower JC, Liu H, Garrison TM, et al. Geochemical and mineralogical evidence for a coal-hosted uranium deposit in the Yili Basin, Xinjiang, northwestern China. Ore Geol Rev 2015;70:1–30.
[44] Dai S, Seredin VV, Ward CR, Hower JC, Xing Y, Zhang W, et al. Enrichment of U-Se–Mo–Re–V in coals preserved within marine carbonate successions: geochemical and mineralogical data from the Late Permian Guiding Coalfield, Guizhou, China. Miner Deposita 2015;50(2):159–86.
[45] Finkelman RB. Modes of occurrence of potentially hazardous elements in coal: levels of confidence. Fuel Process Technol 1994;39(1):21–34.
[46] Huggins FE, Huffman GP. Modes of occurrence of trace elements in coal from XAFS spectroscopy. Int J Coal Geol 1996;32(1–4):31–53.
[47] Wang L, Ju Y, Liu G, Chou C-L, Zheng L, Qi C. Selenium in Chinese coals: distribution, occurrence, and health impact. Environ Earth Sci 2010;60(8):1641–51.
[48] Liu J, Yang Z, Yan X, Ji D, Yang Y, Hu L. Modes of occurrence of highly-elevated trace elements in superhigh-organic-sulfur coals. Fuel 2015;156:190–7.
[49] Ketris MP, Yudovich YE. Estimations of Clarkes for Carbonaceous biolithes: World averages for trace element contents in black shales and coals. Int J Coal Geol 2009;78(2):135–48.
[50] Dai S, Wang X, Seredin VV, Hower JC, Ward CR, O'Keefe JMK, et al. Petrology, mineralogy, and geochemistry of the Ge-rich coal from the Wulantuga Ge ore deposit, Inner Mongolia, China: new data and genetic implications. Int J Coal Geol 2012;90–91:72–99.
[51] Qi Cuicui, Guijian Liu Yu, Kang Ch-Lin Chou, Wang Ruwei. Sequential solvent extraction for forms of antimony in five selected coals. J Geol 2008;116(2):192–200.
[52] Pires M, Fiedler H, Teixeira EC. Geochemical distribution of trace elements in coal: modelling and environmental aspects. Fuel 1997;76(14):1425–37.
[53] Sia S-G, Abdullah WH. Enrichment of arsenic, lead, and antimony in Balingian coal from Sarawak, Malaysia: modes of occurrence, origin, and partitioning behaviour during coal combustion. Int J Coal Geol 2012;101:1–15.
[54] Singh RM, Singh MP, Chandra D. Occurrence, distribution and probable source of the trace elements in Ghugus coals, Wardha valley, districts Chandrapur and Yeotmal, Maharashtra, India. Int J Coal Geol 1983;2(4):371–81.
[55] Ward CR, Spears DA, Booth CA, Staton I, Gurba LW. Mineral matter and trace elements in coals of the Gunnedah Basin, New South Wales, Australia. Int J Coal Geol 1999;40(4):281–308.
[56] Ruppert L, Finkelman R, Boti E, Milosavljevic M, Tewalt S, Simon N, et al. Origin and significance of high nickel and chromium concentrations in Pliocene lignite of the Kosovo Basin, Serbia. Int J Coal Geol 1996;29(4):235–58.
[57] Zhou C, Liu G, Yan Z, Fang T, Wang R. Transformation behavior of mineral composition and trace elements during coal gangue combustion. Fuel 2012;97(2):644–50.

[58] Suárez-Ruiz I, Ward CR. Coal Combustion. In: Suárez-Ruiz I, Crelling JC, editors. Applied Coal Petrology. Burlington: Elsevier; 2008. p. 85–117.
[59] Querol X, Fernández-Turiel J, López-Soler A. Trace elements in coal and their behaviour during combustion in a large power station. Fuel 1995;74(3):331–43.
[60] Stam AF, Meij R, te Winkel H, Eijk RJV, Huggins FE, Brem G. Chromium speciation in coal and biomass co-combustion products. Environ Sci Technol 2011;45(6):2450–6.
[61] Linak WP, Wendt JOL. Toxic metal emissions from incineration: mechanisms and control. Prog Energy Combust Sci 1993;19(2):145–85.
[62] Vejahati F, Xu Z, Gupta R. Trace elements in coal: associations with coal and minerals and their behavior during coal utilization – a review. Fuel 2010;89(4):904–11.
[63] Catalano JG, Huhmann BL, Luo Y, Mitnick EH, Slavney A, Giammar DE. Metal release and speciation changes during wet aging of coal fly ashes. Environ Sci Technol 2012;46(21):11804–12.
[64] Deonarine A, Kolker A, Foster AL, Doughten MW, Holland JT, Bailoo JD. Arsenic speciation in bituminous coal fly ash and transformations in response to redox conditions. Environ Sci Technol 2016;50(11):6099–106.
[65] Zielinski RA, Foster AL, Meeker GP, Brownfield IK. Mode of occurrence of arsenic in feed coal and its derivative fly ash, Black Warrior Basin, Alabama. Fuel 2007;86(4):560–72.
[66] Huffman GP, Huggins FE, Shah N, Zhao J. Speciation of arsenic and chromium in coal and combustion ash by XAFS spectroscopy. Fuel Process Technol 1994;39(1):47–62.
[67] Oboirien BO, Thulari V, North BC. Enrichment of trace elements in bottom ash from coal oxy-combustion: Effect of coal types. Appl Energy 2016;177(Supplement C):81–6.
[68] Bhangare RC, Ajmal PY, Sahu SK, Pandit GG, Puranik VD. Distribution of trace elements in coal and combustion residues from five thermal power plants in India. Int J Coal Geol 2011;86(4):349–56.